Absolute testing of flats by using even and odd functions

Chiayu Ai and James C. Wyant

We describe a modified three-flat method. In a Cartesian coordinate system, a flat can be expressed as the sum of even–odd, odd–even, even–even, and odd–odd functions. The even–odd and the odd–even functions of each flat are obtained first, and then the even–even function is calculated. All three functions are exact. The odd–odd function is difficult to obtain. In theory, this function can be solved by rotating the flat 90°, 45°, 22.5°, etc. The components of the Fourier series of this odd–odd function are derived and extracted from each rotation of the flat. A flat is approximated by the sum of the first three functions and the known components of the odd–odd function. In the experiments, the flats are oriented in six configurations by rotating the flats 180°, 90°, and 45° with respect to one another, and six measurements are performed. The exact profiles along every 45° diameter are obtained, and the profile in the area between two adjacent diameters of these diameters is also obtained with some approximation. The theoretical derivation, experiment results, and error analysis are presented.
Key words: Optical testing, optical flat, absolute testing.

Introduction

In a Fizeau interferometer, two flats face each other and form a cavity. Interference fringes reveal the optical path difference (OPD) of the cavity, and hence the relative flatness. In the traditional three-flat method,[1,2] the flats are compared in pairs. By rotating the flats with respect to each other, the exact profiles along several diameters of each flat are obtained. A method with more flats and more combinations has been proposed.[3] However, with both methods, only the profiles along some straight lines can be solved. Several methods have been proposed to measure the flatness of the entire surface.[4–8] All these methods involve tremendous calculations in the least-squares sense. Thus, the fine structure of the surface tends to disappear.

In our previous paper[9] we modified the tree-flat method and used the symmetry properties of the odd and the even functions, especially when the functions were rotated or flipped, to calculate the entire profile of each flat with eight measurements. The number of measurements was twice that of the traditional three-flat method. In this paper we reduce the number of measurements to six. Again every point of a flat is obtained without using the least-squares method.

The authors are with the Wyko Corporation, 2650 East Elvira Road, Tucson, Arizona 85706.
Received 5 October 1992.
0003-6935/93/254698-08$06.00/0.

Theory

A function $F(x, y)$ in a Cartesian coordinate system can be expressed as the sum of an even–odd, and odd–even, an even–even, and an odd–odd function as follows:

$$F(x, y) = F_{ee} + F_{oo} + F_{oe} + F_{eo}, \tag{1}$$

where

$$\begin{aligned}
F_{ee}(x,y) &= \frac{F(x,y) + F(-x,y) + F(x,-y) + F(-x,-y)}{4},\\
F_{oo}(x,y) &= \frac{F(x,y) - F(-x,y) - F(x,-y) + F(-x,-y)}{4},\\
F_{eo}(x,y) &= \frac{F(x,y) + F(-x,y) - F(x,-y) - F(-x,-y)}{4},\\
F_{oe}(x,y) &= \frac{F(x,y) - F(-x,y) + F(x,-y) - F(-x,-y)}{4}.
\end{aligned} \tag{2}$$

Because the flats are facing each other, one flat is flipped. If two flats are $F(x, y)$ and $G(x, y)$, and the flat $G(x, y)$ is flipped in x, then the OPD that is measured equals $F(x, y) + G(-x, y)$. For convenience, we define two operators $[\ ]^x$ and $[\ ]^\theta$:

Flip in x

$$[F(x,y)]^x = F(-x,y),$$

Rotate θ

$$[F(x,y)]^\theta = F(x\cos\theta - y\sin\theta, x\sin\theta + y\cos\theta). \quad (3)$$

Thus $[F(x, y)]^{180°} = F(-x, -y)$, and $F(x, y) + G(-x, y) = F(x, y) + [G(x, y)]^x$. Applying the two operators to Eq. (1),

$$[F(x,y)]^{180°} = F_{ee} + F_{oo} - F_{oe} - F_{eo},$$
$$[F(x,y)]^x = F_{ee} - F_{oo} - F_{oe} + F_{eo}. \quad (4)$$

A comparison of Eqs. (4) with Eq. (1) shows that the sign changes on the right-hand side. We can make use of this fact that the sign changes after a rotation to solve the odd–even, even–odd, even–even, and odd–odd parts of a flat. In the next section, it is shown that the first three parts can be obtained easily and that the odd–odd part is difficult to solve. To overcome this problem, we analyze the surface profile with a Fourier series. In a polar coordinate system, the profile on a circle centered at the origin is a function of θ and has a period of 360°. A periodic function can be expressed as a Fourier series. It can be shown that for $x^2 + y^2 =$ constant, $F_{oe}(x, y)$, $F_{ee}(x, y)$, $F_{eo}(x, y)$, and $F_{oo}(x, y)$, can be expressed as $\Sigma f_i \cos(i\theta)$, $\Sigma f_j \cos(j\theta)$, $\Sigma f_m \sin(m\theta)$, and $\Sigma f_n \sin(n\theta)$, respectively, where i, m = odd and j, n = even. In general, a Fourier series includes infinite frequencies, and practically only a part of the frequencies can be solved. The profile can only be approximated by the sum of the known components of the Fourier series, and hence the error occurs.

Because the odd–even, even–odd, and even–even parts of a flat can be solved easily, as shown in the next section, here we focus only on $F_{oo}(x, y)$. For the points on a circle centered at the origin, an odd–odd function in a Cartesian coordinate system is an odd function of θ in a polar coordinate system and has a period of 180°. The function $F_{oo}(x, y)$ can be expressed as a Fourier sine series as follows:

$$F_{oo}(x,y) = \sum_{m=1} f_{2m} \sin(2m\theta), \quad (5)$$

where $x^2 + y^2 =$ constant, f_{2m} is the corresponding coefficient, and the indices m are natural numbers. To emphasize that $F_{oo}(x, y)$ has a fundamental frequency of 2 (i.e., a period of 180°), a subscript 2θ is added to $F_{oo}(x, y)$. Thus Eq. (5) can be rewritten as

$$F_{oo} = F_{oo,2\theta} = F_{oo,2odd\theta} + F_{oo,2even\theta}, \quad (6)$$

where

$$F_{oo,2even\theta} = \sum_{m=even} f_{2m} \sin(2m\theta)$$
$$= \sum_{m=1} f_{4m} \sin(4m\theta) = F_{oo,4\theta},$$
$$F_{oo,2odd\theta} = \sum_{m=odd} f_{2m} \sin(2m\theta). \quad (7)$$

The subscripts $2odd\theta$ and $2even\theta$ represent the sum of the odd terms of $F_{oo,2\theta}$ and the sum of the even terms of $F_{oo,2\theta}$, respectively. In Eqs. (7), the subscript 4θ indicates that $F_{oo,2even\theta}$ has a fundamental frequency of 4 (i.e., a period of 90°). Similar to what was done in Eq. (6), $F_{oo,4\theta}$ can be divided into two groups as follows:

$$F_{oo,4\theta} = F_{oo,4odd\theta} + F_{oo,4even\theta}, \quad (8)$$

where

$$F_{oo,4odd\theta} = \sum_{m=odd} f_{4m} \sin(4m\theta),$$
$$F_{oo,4even\theta} = \sum_{m=even} f_{4m} \sin(4m\theta). \quad (9)$$

Therefore an odd–odd function can be expressed as the sum of $nodd\theta$ terms, where n = 2, 4, 8, 16, 32, ... That is

$$F_{oo,2\theta} = F_{oo,2odd\theta} + F_{oo,4odd\theta} + F_{oo,8odd\theta} + F_{oo,16odd\theta} + \ldots, \quad (10)$$

where the $8odd\theta$ and $16odd\theta$ terms are defined as they are in Eqs. (9). It should be noted that each term includes a broad spectrum of the Fourier sine series. For example, $F_{oo,2odd\theta}$ includes the components of $\sin(2\theta)$, $\sin(6\theta)$, $\sin(10\theta)$, $\sin(14\theta)$, etc., and $F_{oo,4odd\theta}$ includes the components of $\sin(4\theta)$, $\sin(12\theta)$, $\sin(20\theta)$, $\sin(28\theta)$, etc. For a smooth surface, the odd–odd part can be well represented by the first two terms of Eq. (10). Applying the rotation operator to Eqs. (6) and (8), it can be shown that

$$[F_{oo,2\theta}]^{90°} = -F_{oo,2odd\theta} + F_{oo,2even\theta}, \quad (11)$$

$$[F_{oo,4\theta}]^{45°} = -F_{oo,4odd\theta} + F_{oo,4even\theta}, \quad (12)$$

where the terms on the right-hand side are defined in Eqs. (7) and (9), respectively. Comparing Eq. (11) with Eq. (6), one can see that the sign of $F_{oo,2odd\theta}$ is opposite. So are the signs of $F_{oo,4odd\theta}$ in Eqs. (12) and (8). In the next section, we show that the $2odd\theta$ and $4odd\theta$ terms can be solved by rotating the flat 90° and 45°, respectively. In theory, the higher-order terms can be derived by rotating the flat at a smaller angle. For example, the $8odd\theta$ term can be determined by rotating the flat 22.5°. Therefore the entire frequencies of the odd–odd part of a flat can be obtained. It should be noted that in this paper, no Fourier series is used to derive the surface. The Fourier series are given here to provide an insight to the limitation of this method. The surface is obtained with simple arithmetic instead.

Algorithm

In this section, we make use of the fact that the sign changes after a rotation to solve the odd–even, even–odd, and even–even parts of a flat first and then the

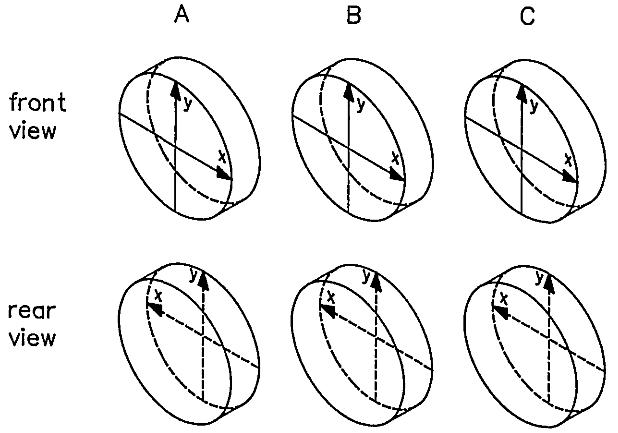

Fig. 1. Three flats, $A(x, y)$, $B(x, y)$, and $C(x, y)$, of a front view and a rear view. The coordinate systems indicate the orientations of the flats.

odd–odd part. Figure 1 shows the three flats, $A(x, y)$, $B(x, y)$, and $C(x, y)$, of a front view and a rear view. The coordinate systems indicate the orientations of the flats. Figure 2 shows the six configurations and the corresponding measurements. In each configuration, the flat above is a flat of a front view, and the flat below is flipped in x and is a flat of a rear view. In some configurations, one flat is rotated 180°, 90°, or 45° with respect to another flat. The equations of the six configurations are

$$M_1 = A + B^x, \qquad M_2 = A^{180°} + B^x,$$
$$M_3 = A^{90°} + B^x, \qquad M_4 = A^{45°} + B^x,$$
$$M_5 = A + C^x, \qquad M_6 = B + C^x. \tag{13}$$

If one uses Eqs. (1) and (4), M_1, M_2, and M_5 can be written as

$$M_1 = A_{ee} + A_{oo} + A_{oe} + A_{eo} + B_{ee} - B_{oo} - B_{oe} + B_{eo},$$
$$M_2 = A_{ee} + A_{oo} - A_{oe} - A_{eo} + B_{ee} - B_{oo} - B_{oe} + B_{eo},$$
$$M_5 = A_{ee} + A_{oo} + A_{oe} + A_{eo} + C_{ee} - C_{oo} - C_{oe} + C_{eo}. \tag{14}$$

Therefore all the odd–even and the even–odd parts of the three flats can be obtained easily as given below:

$$A_{oe} + A_{eo} = (M_1 - M_2)/2,$$
$$B_{oe} + B_{eo} = \{[M_1 - (M_1)^{180°}]/2 - (A_{oe} + A_{eo})\}^x,$$
$$C_{oe} + C_{eo} = \{[M_5 - (M_5)^{180°}]/2 - (A_{oe} + A_{eo})\}^x. \tag{15}$$

To cancel all with the odd–even and the even–odd parts from M_1, M_5, and M_6, one can rotate the data 180° with the rotation operation defined in Eqs. (4). We define m_1, m_5, and m_6 as

$$m_1 = [M_1 + (M_1)^{180°}]/2 = A_{ee} + A_{oo} + B_{ee} - B_{oo},$$
$$m_5 = [M_5 + (M_5)^{180°}]/2 = A_{ee} + A_{oo} + C_{ee} - C_{oo},$$
$$m_6 = [M_6 + (M_6)^{180°}]/2 = B_{ee} + B_{oo} + C_{ee} - C_{oo}. \tag{16}$$

It should be noted that m_1, m_5, and m_6 include only even–even and odd–odd functions. From Eqs. (16), all the even–even parts can be derived easily as given below:

$$A_{ee} = [m_1 + m_5 - m_6 + (m_1 + m_5 - m_6)^x]/4,$$
$$B_{ee} = [m_1 + (m_1)^x - 2A_{ee}]/2,$$
$$C_{ee} = [m_5 + (m_5)^x - 2A_{ee}]/2. \tag{17}$$

Now all the odd–even, even–odd, and even–even parts of the three flats are obtained. If we subtract

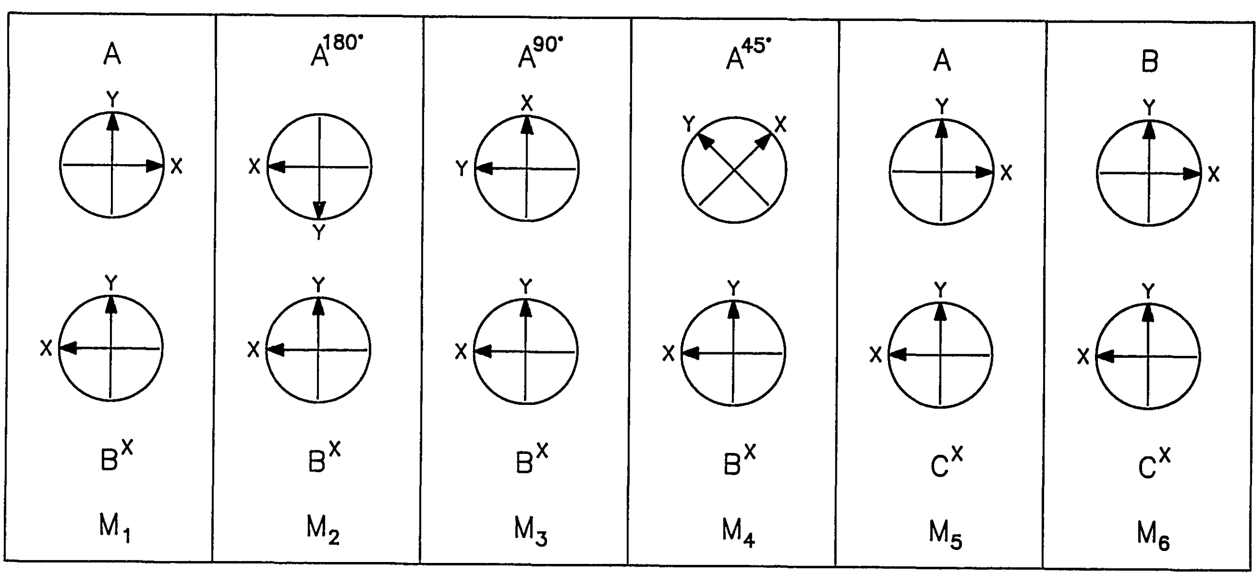

Fig. 2. Six configurations and the corresponding measurements. In each configuration, the flat below is flipped in x and is a flat of a rear view.

the known even–even parts from Eqs. (16), the three new equations include only the odd–odd parts and are linearly dependent. Therefore the odd–odd parts cannot be solved exactly. From Eq. (6), the three odd–odd functions, $A_{oo}(x, y)$, $B_{oo}(x, y)$, and $C_{oo}(x, y)$, have a fundamental frequency of 2 and can be expressed as

$$\begin{aligned} A_{oo} &= A_{oo,2\theta} = A_{oo,2\text{odd}\theta} + A_{oo,2\text{even}\theta}, \\ B_{oo} &= B_{oo,2\theta} = B_{oo,2\text{odd}\theta} + B_{oo,2\text{even}\theta}, \\ C_{oo} &= C_{oo,2\theta} = C_{oo,2\text{odd}\theta} + C_{oo,2\text{even}\theta}, \end{aligned} \tag{18}$$

where all 2oddθ and 2evenθ terms are defined in the same way as in Eqs. (7). Similarly,

$$\begin{aligned} (A_{oo,2\theta})^{90^\circ} &= -A_{oo,2\text{odd}\theta} + A_{oo,2\text{even}\theta}, \\ (B_{oo,2\theta})^{90^\circ} &= -B_{oo,2\text{odd}\theta} + B_{oo,2\text{even}\theta}, \\ (C_{oo,2\theta})^{90^\circ} &= -C_{oo,2\text{odd}\theta} + C_{oo,2\text{even}\theta}. \end{aligned} \tag{19}$$

If a flat has only the odd–odd component, the 2oddθ term can be obtained easily by subtracting two measurements that are obtained before and after the flat is rotated 90° with respect to the other flat, such as M_1 and M_3. Because of the subtraction, the contribution of the surface not rotated is removed, the 2evenθ term of the rotated surface is canceled, and only the 2oddθ term remains. This is equivalent to the technique that opticians have used for years to determine the astigmatic error of a flat.

Because all of the even–even, even–odd, and odd–even parts of each flat are obtained, we can subtract them from M_1, M_3, and M_6, respectively. Define m_1', m_3', and m_6' from Fig. 2 as follows:

$$\begin{aligned} m_1' &= M_1 - (A_{oe} + A_{eo} + A_{ee}) - (B_{oe} + B_{eo} + B_{ee})^x, \\ m_3' &= M_3 - (A_{oe} + A_{eo} + A_{ee})^{90^\circ} - (B_{oe} + B_{eo} + B_{ee})^x, \\ m_6' &= M_6 - (B_{oe} + B_{eo} + B_{ee}) - (C_{oe} + C_{eo} + C_{ee})^x. \end{aligned} \tag{20}$$

The above equations can be simplified as given below:

$$\begin{aligned} m_1' &= A_{oo} - B_{oo}, \\ m_3' &= (A_{oo})^{90^\circ} - B_{oo}, \\ m_6' &= B_{oo} - C_{oo}, \end{aligned} \tag{21}$$

where $A_{oo} = A_{oo,2\theta}$, $B_{oo} = B_{oo,2\theta}$, and $C_{oo} = C_{oo,2\theta}$. It should be noted that Eqs. (21) includes only the odd–odd part of each flat. By substituting Eqs. (18) and (19) into Eqs. (21) and by using the 90° rotation operation, all the 2oddθ parts of the three flats are obtained as given below[10]:

$$\begin{aligned} A_{oo,2\text{odd}\theta} &= (m_1' - m_3')/2, \\ B_{oo,2\text{odd}\theta} &= [(m_1')^{90^\circ} - m_3']/2, \\ C_{oo,2\text{odd}\theta} &= [(m_6')^{90^\circ} - m_6' + (m_1')^{90^\circ} - m_3']/2. \end{aligned} \tag{22}$$

According to Eqs. (7) and (8), the 2evenθ term of Eqs. (18) has a frequency of 4 and can be divided into two halves: 4evenθ and 4oddθ terms. By using a similar procedure for deriving Eqs. (20)–(22), the 4oddθ term can be obtained by rotating one flat 45° instead of 90°. From M_1, M_4, and M_6 of Fig. 2, we define m_1'', m_4'', and m_6'' as

$$\begin{aligned} m_1'' &= M_1 - (A_{oe} + A_{eo} + A_{ee} + A_{oo,2\text{odd}\theta}) \\ &\quad - (B_{oe} + B_{eo} + B_{ee} + B_{oo,2\text{odd}\theta})^x, \\ m_4'' &= M_4 - (A_{oe} + A_{eo} + A_{ee} + A_{oo,2\text{odd}\theta})^{45^\circ} \\ &\quad - (B_{oe} + B_{eo} + B_{ee} + B_{oo,2\text{odd}\theta})^x, \\ m_6'' &= M_6 - (B_{oe} + B_{eo} + B_{ee} + B_{oo,2\text{odd}\theta}) \\ &\quad - (C_{oe} + C_{eo} + C_{ee} + C_{oo,2\text{odd}\theta})^x. \end{aligned} \tag{23}$$

The above equations can also be simplified as given below:

$$\begin{aligned} m_1'' &= A_{oo,4\theta} - B_{oo,4\theta}, \\ m_4'' &= (A_{oo,4\theta})^{45^\circ} - B_{oo,4\theta}, \\ m_6'' &= B_{oo,4\theta} - C_{oo,4\theta}. \end{aligned} \tag{24}$$

By using Eq. (12), all the 4oddθ terms from Eqs. (12) and (24) can be obtained as given below:

$$\begin{aligned} A_{oo,4\text{odd}\theta} &= (m_1'' - m_4'')/2, \\ B_{oo,4\text{odd}\theta} &= [(m_1'')^{45^\circ} - m_4'']/2, \\ C_{oo,4\text{odd}\theta} &= [(m_6'')^{45^\circ} - m_6'' + (m_1'')^{45^\circ} - m_4'']/2. \end{aligned} \tag{25}$$

Therefore for the odd–odd part of a flat, the sum of one half of the Fourier sine series (i.e., the 2oddθ term) is obtained from the 90° rotation group. The other half is further divided into two halves, and one of them (i.e., the 4oddθ term) is obtained from the 45° rotation group. After each rotation, one half of the unknown components of the Fourier sine series of the odd–odd function is obtained. In theory, the higher-order terms can be derived by rotating the flat at a smaller angle. For example, the 8oddθ term can be determined by rotating the flat 22.5°. Therefore the entire frequencies of the odd–odd part of a flat and hence the entire surface are obtained. In practice, a rotation angle of less than 45° may cause errors in the measurement results, because of the difficulty in the interpolation for the points that are not on the nodes of the square gride and because of the lengthy measurement period.

In summary, if the odd–odd parts of the surfaces can be approximated by 2oddθ and 4oddθ terms, the six-measurement algorithm recovers the flats, and the three flats can be approximated by the equations below:

$$\begin{aligned} A &= A_{ee} + A_{oe} + A_{eo} + A_{oo,2\text{odd}\theta} + A_{oo,4\text{odd}\theta}, \\ B &= B_{ee} + B_{oe} + B_{eo} + B_{oo,2\text{odd}\theta} + B_{oo,4\text{odd}\theta}, \\ C &= C_{ee} + C_{oe} + C_{eo} + C_{oo,2\text{odd}\theta} + C_{oo,4\text{odd}\theta}, \end{aligned} \tag{26}$$

where all the terms on the right-hand side are obtained from Eqs. (15), (17), (22), and (25). It should be noted that those four equations use simple arithmetic without a Fourier transform or least squares. The algorithm of this modified three-flat method is summarized and given in the following list:

1. The six measurements according to Fig. 2.
2. $A_{oe} + A_{eo}$, $B_{oe} + B_{eo}$, and $C_{oe} + C_{eo}$ from Eq. (15).
3. A_{ee}, B_{ee}, and C_{ee} from Eqs. (16) and (17).
4. The 2oddθ term of each flat, obtained from Eqs. (20) and (22).
5. The 4oddθ term of each flat, obtained from Eqs. (23) and (25).
6. The flats approximated by Eq. (26).

Simulation

In simulation, the six measurements can be generated from three hyperthetic flats. The three flats are then reconstructed with the algorithm. The component of the highest angular frequency in the first 36 Zernike polynomials[11] is $\sin(4\theta)$. When the three hyperthetic flats are originally generated by using the first 36 Zernike polynomials, the three reconstructed flats are exactly equal to the three original hyperthetic flats, except for the errors resulting from limited quantization levels. This shows that the six-measurement algorithm recovers the flats as long as the odd–odd parts of the surfaces can be approximated by 2oddθ and 4oddθ terms. If the three hyperthetic flats are generated from higher-order Zernike polynomials, all the even–even, even–odd, odd–even, 2oddθ, and 4oddθ terms can still be recovered. However, the reconstructed surface is missing all $\sin(8n\theta)$ terms, where $n = 1, 2, 3, \ldots$. To recover the higher-order terms, more measurements with a smaller rotation angle are needed.

Although both 2oddθ and 4oddθ terms include a broad spectrum of the Fourier sine series, the two terms do not cover the entire spectrum, and hence the error occurs when a surface has a white spectrum, such as the spectrum of a steep spike. If we let one of the three hyperthetic flats, for instance flat C, have a local error, then its reconstructed flat C′ has some errors. Figure 3 shows that flat C has a Gaussian shape bump, 1λ peak to valley (pv), centered at (0.87, 33.75°) in a polar coordinate system, where the pupil of flat C defines a unit circle. The full width at $1/e$ of the bump is 20% of the pupil diameter. The shape of this bump is difficult to represent with Zernike polynomials. The fit error is 0.063λ (rms) and 0.674λ (pv). Flat C′ reconstructed with the six-measurement algorithm and flat C″ obtained from the first 36 Zernike polynomials are also shown in Fig. 3. Flat C′ shows a ripple of $\sin(8\theta)$. A comparison of flat C′ with flat C shows that the ripple is 0.024λ (rms) and 0.110λ (pv). It should be noted that with the proposed algorithm, if the width of the bump is wider or the center of the bump is not at m*11.25°, m = odd integer, the error of flat C′ is much smaller or even equal to zero.

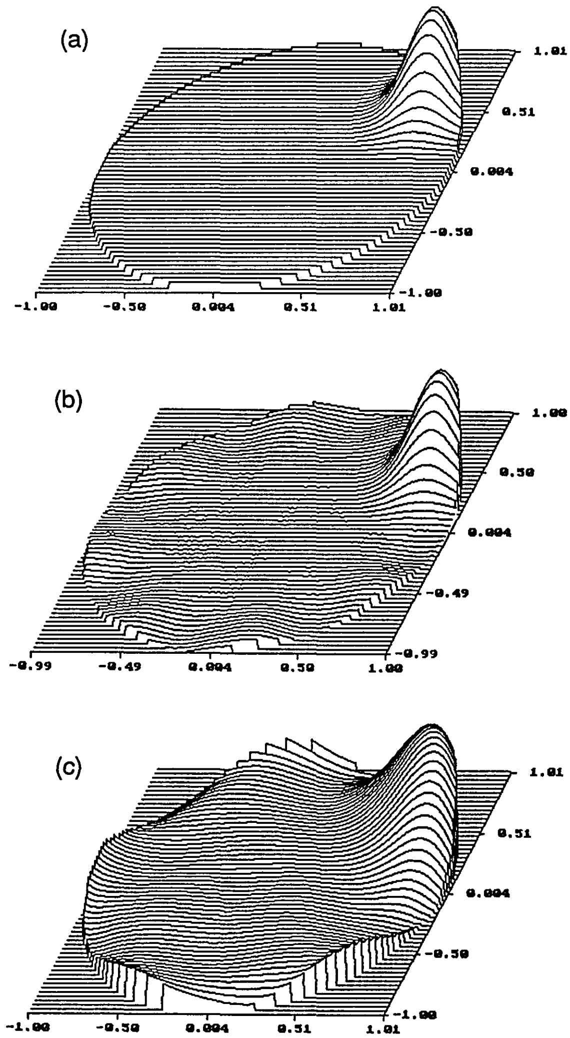

Fig. 3. Simulation results: (a) flat C has a Gaussian shape bump of 1λ (pv); (b) Reconstructed flat C′, where the ripple = 0.11λ (pv); (c) flat C″, obtained from the first 36 Zernike polynomials of flat C.

Experiment

Figure 4 is the experimental setup of a phase-shifting Fizeau interferometer with a source at 632.8 nm. The two flats A and B face each other and form a cavity. Flat B is flipped in the horizontal direction

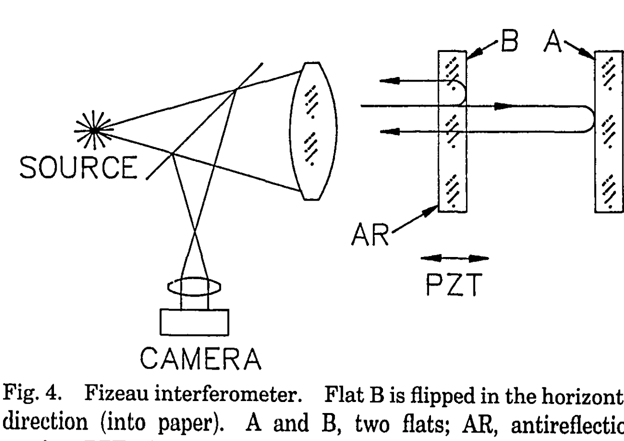

Fig. 4. Fizeau interferometer. Flat B is flipped in the horizontal direction (into paper). A and B, two flats; AR, antireflection coating; PZT, piezoelectric transducer.

(into the paper). The back surface of flat B is polished and has an antireflection coating. Flat B is shifted by a piezoelectric transducer. The phase-shifting interferograms are detected by a video camera, and the OPD of the cavity is calculated.[12] From this configuration, M_1 of Eqs. (13) is obtained. Similarly, the other five measurements are obtained by placing the flats according to Fig. 2. Figure 5 is the OPD maps of the six measurements. The data array of each flat has a size of 286 × 286. The six arrays are then inserted into the algorithm to calculate the three flats. It takes roughly 100 s to calculate with a 486 computer. Figure 6 is the surface profiles of the three flats derived. It is clear that there are two spikes in flat B, in about the 11 o'clock direction. In Fig. 5, under close examination, we can see these two spikes at the corresponding locations in M_{1-6}, i.e., in roughly the 1 o'clock direction in M_1, M_2, M_3, and M_4, and in roughly the 11 o'clock direction in M_6. (These spikes can be seen easily in a scanning map, which is not shown here, but the spikes are not so obvious in Fig. 5.) This clearly shows that the fine structure of a flat is preserved and can be seen with this algorithm. In Figs. 5 and 6 it should be noted

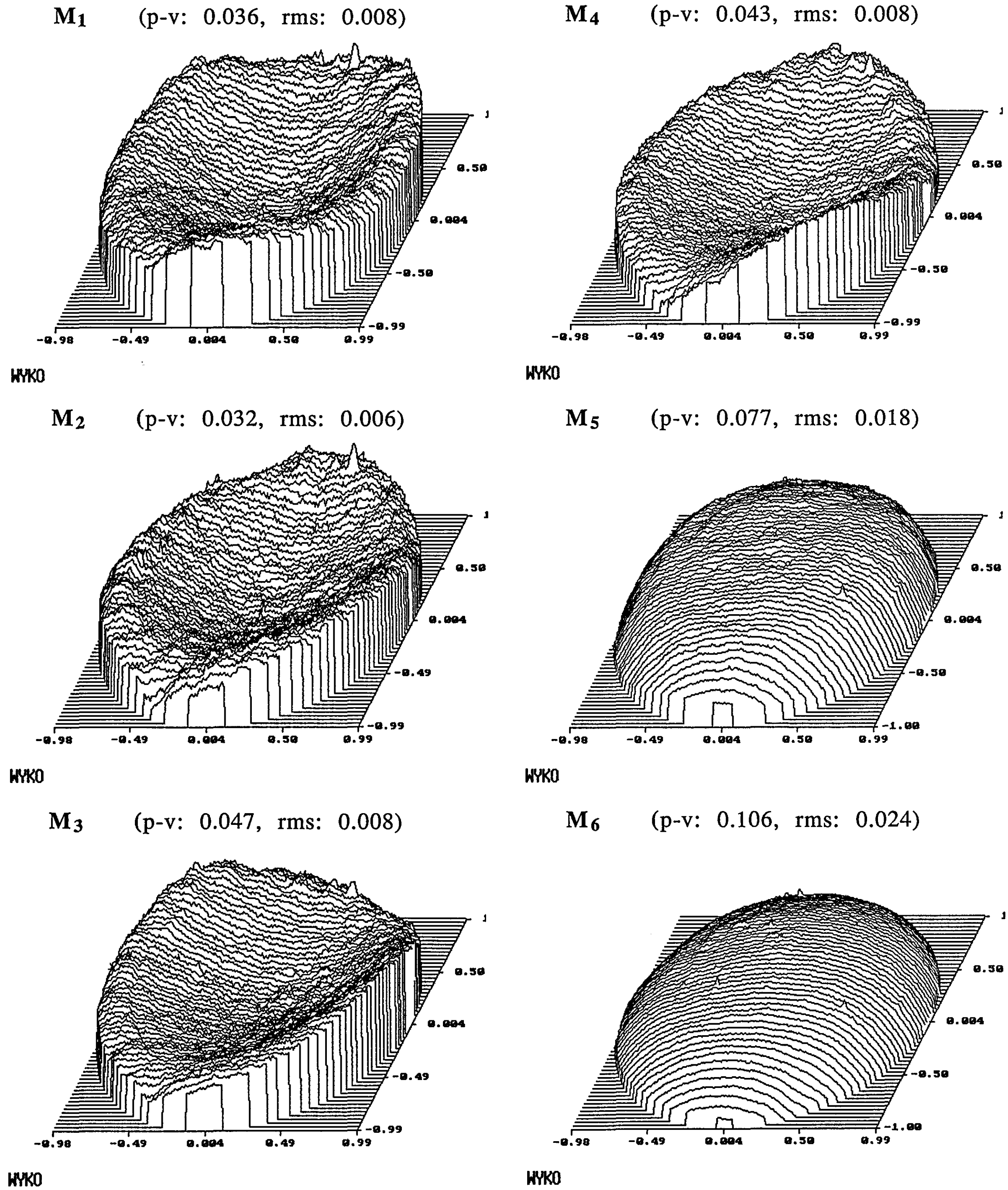

Fig. 5. (a)–(f), Optical path difference maps (in waves) of the six measurements, where M_i's correspond to those in Fig. 2.

Flat A (p-v:0.0420, rms:0.0089)

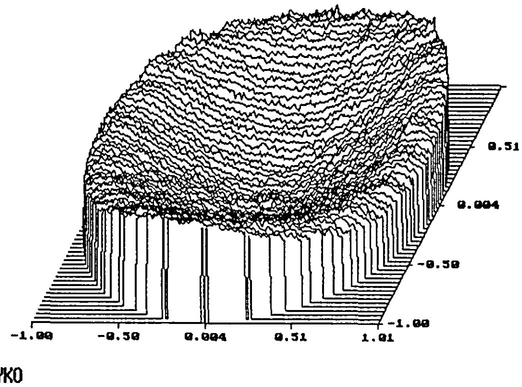

Flat B (p-v:0.0313, rms:0.0034)

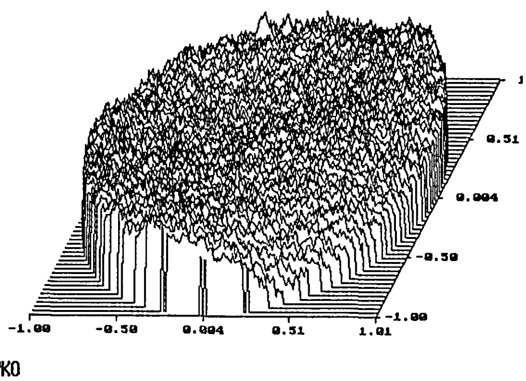

Flat C (p-v:0.1123, rms:0.0232)

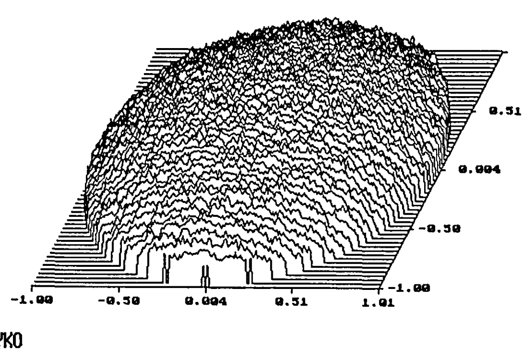

Fig. 6. (a)–(c) Surface profiles (in waves) of flats A, B, and C derived from six measurements in Fig. 5.

that the pv value and the vertical scales vary from figure to figure. Flat B of Fig. 6 is so flat (0.0313λ pv, 0.0034λ rms) that the noise dominates, and no obvious feature can be seen in this figure.

Discussion

To analyze the error, the data arrays of the three flats in Fig. 6 are inserted into Eqs. (13) to generate six reconstructed measurements. Using the same algorithm, we reobtain profiles of the three flats. The three reobtained or reconstructed flats are similar to their corresponding flats in Fig. 6. The difference between two corresponding flats is small and close to the quantization error of the interferometer.

However, the difference between the two corresponding measurements of the six measurements and the six reconstructed measurements is not small. In theory, if the flats and the environment remain unchanged during the multiple measurements, the two corresponding measurements should have no difference. This difference represents the measurement reproducibility error, which is mainly due to the changes in the environment during the long period of measurements and the changes of the surfaces during the rotation manipulation. This error can also be observed by the following procedure. First perform a measurement with two flats. Then remove the flats, replace them in the original orientation, and perform a second measurement. The difference between the two measurements is the measurement reproducibility error. For an environment that is not well controlled, this is the dominating error source compared with other error sources as described below.

Because both 2oddθ and 4oddθ terms include a broad spectrum of the Fourier sine series, the fine structure on a test flat can be seen in the resulting surface. However, because the two terms do not include the entire spectrum of the Fourier series, the reconstructed surface may have errors. This error is prominent for a flat with steep spikes, as shown in Fig. 3. Moreover, the rotation operation $[\ ]^{45°}$ in Eqs. (23) and (25) requires interpolation for the points not on the nodes of a square grid array. This may also introduce small errors. The decentering of the rotation and the flip operations may be another error source. In experiments, the six measurements have different tilts and pistons. Because the tilt and the piston are not of interest, they can be subtracted from Eqs. (13) or (15). This does not affect the rest of the equations. From the experiments, we find that the measurement reproducibility error is the major limiting factor of the accuracy of this method. For the three flats, there are four basic configurations.[4] However, this method has six measurements. It becomes an overconstrained condition, and one can use an iteration method to reduce this measurement reproducibility error.

It is interesting to compare this method with the traditional three-flat method. If the flat is shrunk to a straight-line body along the y-axis, only four out of the set of six measurements are left, as follows:

$$\begin{aligned} M_1 &= A + B^x = A(y) + B(y), \\ M_2 &= A^{180°} + B^x = A(-y) + B(y), \\ M_5 &= A + C^x = A(y) + C(y), \\ M_6 &= B + C^x = B(y) + C(y). \end{aligned} \tag{27}$$

From M_1, M_5, and M_6, we are able to solve $A(y)$, $B(y)$, and $C(y)$. This resembles the traditional three-flat-method result. It can be shown that for a two-dimensional flat, if only the profiles along the diameters are of interest, the four measurements, M_1, M_4, M_5, and M_6, are necessary for solving the exact profiles along the diameter of every 45° angle. No approximation is used for these diameters; the profiles along the diameters are obtained exactly, regardless of the profile of the flat. Adding two more measurements, the profile in the area between two adjacent diameters of these diameters is also obtained with some approximation; i.e., the odd–odd part of a flat is approximated by 2oddθ and 4oddθ terms. The other three parts are obtained exactly. If a measurement with a smaller rotation angle is taken, the higher-order component can be obtained. In theory, if the angle is infinitesimal, all the components, and hence the exact profile of the entire flat, can be acquired.

Conclusion

Using the symmetry properties of odd and even functions, the flat is decomposed to four components: odd–even, even–odd, even–even, and odd–odd. The first three are obtained easily. The odd–odd one can be analyzed as a Fourier sine series and is divided into several groups. For a flat, the higher frequency components of the Fourier series are small in general. The odd–odd function can be well approximated by the 2oddθ and the 4oddθ terms. It should be noted that the 2oddθ and the 4oddθ terms are obtained with simple arithmetic instead of a Fourier transform.

In conclusion, the flat is calculated using simple arithmetic without a Fourier series expansion, least squares, or a Zernike fit. With six measurements, the profiles along the four diameters of a flat are exact: 0°, 45°, 90°, and 135°. The relationship among these profiles is also defined exactly. Because the flat is approximated by the sum of the odd–even, even–odd, and even–even functions and the known components of the odd–odd function, the area between two adjacent diameters is missing $\sin(8n\theta)$ components, where $n = 1, 2, 3, \ldots$. These higher-order terms can be derived by rotating the flats at smaller angles. As long as the odd–odd parts of the surfaces can be approximated by 2oddθ and 4oddθ terms, the six-measurement algorithm can be used to measure the flats.

We thank Lianzhen Shao of Tucson Optical Research Corporation in Tucson, Arizona, for pointing out the redundancy of the eight measurements and suggesting six measurements.

References and Notes

1. G. Schulz, "Ein interferenzverfahren zur absolute ebnheitsprufung langs beliebiger zntralschnitte," Opt. Acta **14,** 375–388 (1967).
2. G. Schulz and J. Schwider, "Interferometric testing of smooth surfaces," in *Progress in Optics XIII,* E. Wolf, ed., (North-Holland, Amsterdam, 1976), Chap. 4.
3. J. Schwider, "Ein interferenzverfahren zur absolutprufung von planflachennormalen. II," Opt. Acta **14,** 389–400 (1967).
4. B. S. Fritz, "Absolute calibration of an optical flat," Opt. Eng. **23,** 379–383 (1984).
5. J. Grzanna and G. Schulz, "Absolute testing of flatness standards at square-grid points," Opt. Commun. **77,** 107–112 (1990).
6. C. Ai, H. Albrecht, and J. C. Wyant, "Absolute testing of flats using shearing technique," in *Annual Meeting,* Vol. 17 of 1991 OSA Technical Digest Series (Optical Society of America, Washington, D.C., 1991), paper WN1.
7. J. Grzanna and G. Schulz, "Absolute flatness testing by the rotation method with optimal measuring error compensation," Appl. Opt. **31,** 3767–3780 (1992).
8. W. Primak, "Optical flatness standard II: reduction of interferograms, "in *Optical Testing and Metrology II,* C. P. Grover, ed., Proc. Soc. Photo-Opt. Instrum. Eng. **954,** 375–381 (1989).
9. C. Ai and J. C. Wyant, "Absolute testing of flats decomposed to even and odd functions," in *Interferometry: Applications,* R. J. Pryputniewicz, ed., Proc. Soc. Photo-Opt. Instrum. Eng., **1776,** 73–83 (1992).
10. It is straightforward that from Eqs. (13), we have $M_1 - M_3 = A - A^{90°}$. Therefore, the contribution of B is completely removed, regardless the resulting profile of B, and hence $A_{oo,2odd\theta}$ can be derived. Similarly, $(M_1)^{90°} - M_3 = (B^x)^{90°} - B^x$, and the contribution of A is completely canceled, and $B_{oo,2odd\theta}$ is obtained. In our previous paper,[9] there were eight measurements, and the derivation of $C_{oo,2odd\theta}$ was similar to that given above. With the eight-measurement algorithm, because of the subtraction, the contribution of the surface that is not rotated is removed. The measurement error of a surface does not affect the other two surfaces. However, in this six-measurement algorithm, it is not so simple. From Eqs. (13),

$$(M_6)^{90°} - M_6 + (M_1)^{90°} - M_3 = (C^x)^{90°} - C^x + (B)^{90°} + (B^x)^{90°} - B - B^x. \quad \text{(A1)}$$

Again the contribution of A is completely deleted. Because only the odd–odd part is unknown, we only consider this part by subtracting the odd–even, even–odd, and even terms from each term in Eq. (A1). Therefore, all B terms of Eq. (A1) become

$$(B_{oo})^{90°} + [(B_{oo})^x]^{90°} - B_{oo} - (B_{oo})^x = 0. \quad \text{(A2)}$$

After the subtraction, Eq. (A1) is the same as Eqs. (22). This substration operation is equivalent to applying an odd–odd operation to Eq. (A1) to filter non-odd–odd terms.
11. D. Malacala, ed., "Zernike polynomials and wavefront fitting," in *Optical Shop Testing,* (New York, 1978), 489–505.
12. K. Creath, "Phase-measurement interferometry techniques," in *Progress in Optics XXVI,* E. Wolf, ed. (North-Holland, Amsterdam, 1988), 349–393.